Eur. Phys. J. A **9**, 13–17 (2000)

THE EUROPEAN PHYSICAL JOURNAL A

Short note

The A = 51 mirror nuclei ^{51}Fe and ^{51}Mn

J. Ekman[1,a], D. Rudolph[1], C. Fahlander[1], R.J. Charity[2], W. Reviol[2], D.G. Sarantites[2], V. Tomov[2], R.M. Clark[3], M. Cromaz[3], P. Fallon[3], A.O. Macchiavelli[3], M. Carpenter[4], and D. Seweryniak[4]

[1] Department of Physics, Lund University, S-22100 Lund, Sweden
[2] Chemistry Department, Washington University, St. Louis, MO 63130, USA
[3] Nuclear Science Division, Lawrence Berkeley National Laboratory, Berkeley, CA 94720, USA
[4] Physics Division, Argonne National Laboratory, Argonne, IL 60439, USA

Received: 20 July 2000 / Revised version: 28 July 2000
Communicated by D. Schwalm

Abstract. Eighteen previously unknown γ-ray transitions were identified in the $T_z = -1/2$ nucleus ^{51}Fe following the fusion-evaporation reaction ^{32}S(^{28}Si,2α1n)^{51}Fe. The level scheme reaches the fully aligned $I^\pi = 27/2^-$ terminating state of the five holes in the $f_{7/2}$ shell. The $17/2^-$ state was found to be isomeric, and the lifetime was measured to be 2.87 ns. The mirror symmetry of ^{51}Fe and ^{51}Mn is discussed, and the level scheme of ^{51}Fe is compared to shell-model calculations.

PACS. 23.20.Lv Gamma transitions and level energies – 21.10.Sf Coulomb energies – 21.10.Tg Lifetimes – 27.40.+z $39 \leq A \leq 58$

The study of mirror nuclei in the $f_{7/2}$ shell is of considerable interest. Due to the fact that the number of protons and neutrons are interchanged in mirror nuclei, one expects similar level schemes with differences only due to Coulomb interaction. The investigation of mirror nuclei is therefore an unique source for the understanding of how Coulomb interaction may affect single-particle wave functions. Recently, it has become possible to perform shell-model calculations within the full fp space up to mass $A = 52$ nuclei [1], whereas the upper limit for extensive experimental studies of mirror nuclei is at $A = 49$ [2,3]. Only a few mirror states are known for $A = 53$ [4] and $A = 55$ [5]. ^{51}Mn has previously been investigated in terms of high-spin γ-ray spectroscopy [6–8]. The $I^\pi = 27/2^-$ terminating state has been reached, which corresponds to the complete spin alignment of the five $f_{7/2}$ holes with respect to the doubly-magic ^{56}Ni core. The lifetime of the $17/2^-$ state in ^{51}Mn has been measured to 2.2(3) ns [9]. The ground state spin and parity of ^{51}Fe has been deduced to $I^\pi = 5/2^-$ and suggestions have been made for a few excited low-spin states by means of a ^{54}Fe(^{3}He,^{6}He)^{51}Fe reaction [10]. Independent of our study, Bentley *et al.* [11] report on excited states in ^{51}Fe at the same time.

The present study employed a ^{32}S+^{28}Si fusion-evaporation reaction. The 99.1% enriched 0.5 mg/cm^2 thin ^{28}Si target was supported by a 1 mg/cm^2 Au foil, which faced the 130 MeV ^{32}S beam from the Argonne Tandem-Linac Accelerator System (ATLAS). The γ-rays were detected in the Gammasphere array [12], which at the time of the experiment comprised 78 Ge-detectors. The Heavymet collimators were removed to allow γ-ray multiplicity and sum-energy measurements [13]. Evaporated charged particles were detected in the 4π CsI-array Microball [14]. The dedicated Neutron Shell [15] was used for the first time in this experiment to detect evaporated neutrons. It consists of 30 liquid scintillators and replaces the Ge-detectors in the most forward section of Gammasphere, covering about 1π solid angle. Gamma-rays detected in coincidence with charged particles and neutrons provide reaction channel selection, which is further improved by applying the total energy plane selection method [16]. Data was written to magnetic tape either if one neutron and at least two γ-rays or if at least three γ-rays were detected.

The events were sorted into various E_γ projections to correlate the emitted γ-rays with the appropriate reaction channel. The $A = 51$ mirror nuclei ^{51}Fe and ^{51}Mn were populated in the 2α1n- and 2α1p-channel, respectively. Figure 1(a) shows the cleaned 2α1n-gated spectrum. Contaminating lines have been subtracted from the raw 2α1n-gated projection. These lines originated from i) the 2α1p1n-channel ^{50}Mn (if the proton escaped the detection in Microball), ii) from ^{51}Mn (due to neutron-γ misidentification and reactions on small ^{29}Si target impurities), and iii) from ^{52}Mn (due to proton-α misidentification and reactions on small ^{30}Si target impurities). The spectrum in fig. 1(b) is the cleaned 2α1p-gated spectrum

[a] e-mail: jorgen@gamma.kosufy.lu.se

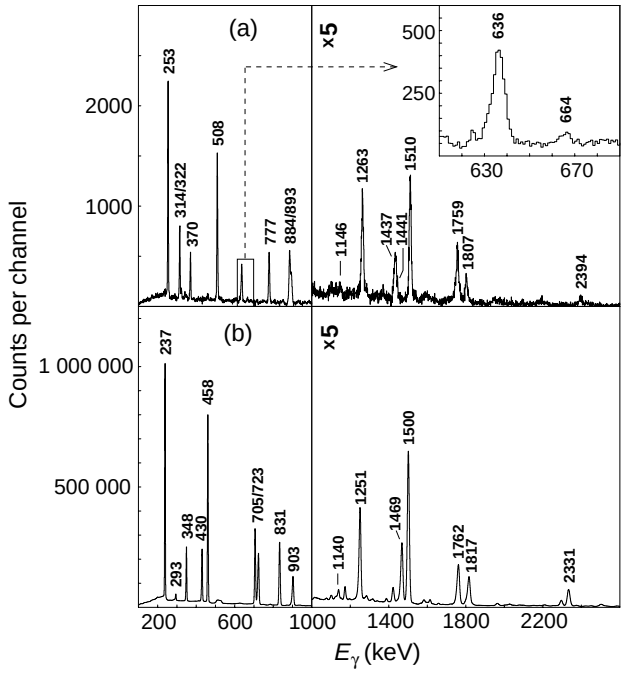

Fig. 1. Part (a) shows the cleaned $2\alpha 1n$-gated spectrum, part (b) the cleaned $2\alpha 1p$-gated spectrum. The inset magnifies the cleaned $2\alpha 1n$-gated spectrum around 650 keV.

providing transitions from ^{51}Mn. Figures 1(a) and (b) readily exhibit great similarities, especially at energies above 1 MeV. Therefore, it is easy to identify the corresponding mirror transitions. The difference in counting statistics in the two spectra is striking. This relates to the relative production cross-sections, namely 0.07% for ^{51}Fe and 18% for ^{51}Mn. The effective efficiencies for protons, α-particles, and neutrons of our data set are 64(4)%, 47(7)% and 50(5)%, respectively. The level scheme of ^{51}Fe is shown in fig. 2(b) and was obtained by investigating sum-energy and intensity relations in the spectrum of fig. 1(a), later on confirmed by $\gamma\gamma$-correlations. For comparison, fig. 2(c) provides the relevant part of a new extensive level scheme of ^{51}Mn [17]. It is in agreement with previous measurements [6–8].

Spins and parities were assigned for states in ^{51}Fe from ratios of yields R_{150-97}, which is the ratio of γ-ray intensities measured at the backward section of Gammasphere ($\overline{\theta} = 150^\circ$ with respect to the beam axis) *versus* the central section of Gammasphere ($\overline{\theta} = 97^\circ$) [18]. Table 1 shows R_{150-97} together with level energies, γ-ray transition energies, relative γ-ray intensities, spin differences, and spins and parities of initial and final states. The relative γ-ray intensities are corrected for angular distribution effects. Due to insufficient statistics, we were not able to deduce R_{150-97} for the 664 keV and 1441 keV transitions. The 664 keV line, shown in the inset of fig. 1(a), is in strong coincidence with the 777 keV transition. The 1441 keV line, however, is not in coincidence with the 777 keV transition but with the other strong transitions in ^{51}Fe. They decay from a state at 7932 keV to which we tentatively assign

Table 1. Energies of excited states in ^{51}Fe, transition energies, relative intensities, angular distribution ratios, and spin differences of the γ-rays placed in the level scheme, and the spins and parities of the initial and final states.

E_x (keV)	E_γ (keV)	$I_{\rm rel}$ (%)	R_{150-97}	ΔI	I_i^π ($\hbar$)	I_f^π ($\hbar$)
253.3(5)	253.3(5)	100(3)	0.64(4)	1	$7/2^-$	$5/2^-$
1146(2)	893(2)	42(2)	0.62(5)	1	$9/2^-$	$7/2^-$
	1146(3)	5(1)		2	$9/2^-$	$5/2^-$
1516(2)	370.0(5)	27(2)	0.55(5)	1	$11/2^-$	$9/2^-$
	1263(1)	61(3)	1.15(9)	2	$11/2^-$	$7/2^-$
2953(3)	1437(4)	40(2)	0.39(5)	1	$13/2^-$	$11/2^-$
	1807(5)	26(2)	1.39(15)	2	$13/2^-$	$9/2^-$
3275(3)	322.3(9)	6(1)	0.69(25)	1	$15/2^-$	$13/2^-$
	1759(3)	54(3)	1.01(9)	2	$15/2^-$	$11/2^-$
3589(3)	314.0(5)	39(2)	0.70(7)	1	$17/2^-$	$15/2^-$
	636.3(7)	43(2)	1.03(8)	2	$17/2^-$	$13/2^-$
4098(3)	508.2(3)	98(3)	0.74(5)	1	$19/2^-$	$17/2^-$
5608(3)	1510.0(8)	75(3)	0.84(6)	1	$21/2^-$	$19/2^-$
6492(3)	883.9(5)	72(3)	0.66(5)	1	$23/2^-$	$21/2^-$
	2394(1)	17(2)		2	$23/2^-$	$19/2^-$
7269(3)	777.2(4)	58(2)	1.26(7)	2	$27/2^-$	$23/2^-$
7933(4)	664(2)	4(2)		(1)	$(25/2^-)$	$27/2^-$
	1441(3)	9(5)		(1)	$(25/2^-)$	$23/2^-$

$I^\pi = (25/2^-)$ based on the mirror symmetry. The lack of statistics did not allow for polarisation measurements, but the negative parity can be assigned to all states assuming $E2$ character for the stretched $\Delta I = 2$ transitions and evidence from mirror symmetry.

The experimental set-up with a thin target, no backing material, and the removed Heavymet collimators allowed for an unusual way of measuring lifetimes of nanosecond isomeric states. Figure 3(a) shows a Ge-detector located at 90° with respect to the beam axis. Assuming an isomeric state, the residual nuclei cover a certain distance x before decaying via γ-ray emission. This means that the angle θ is effectively larger than 90°, which implies that the emitted γ-ray is Doppler shifted towards a lower energy according to $E = E_0(1 + v/c \cdot \cos\theta)$. For reasonably small values of x, the approximation

$$\cos\theta = -\frac{x}{\sqrt{x^2 + d^2}} \approx -\frac{x}{d} \qquad (1)$$

is valid (see fig. 3(a)). One thus obtains the following expression for the energy shift as a function of time:

$$\Delta E = E - E_0 = -E_0 \frac{v^2}{cd} t \; . \qquad (2)$$

The result, schematically shown in fig. 3(b), is a Gaussian distribution with a low energy tail. This distribution is a sum of superpositioned Gaussian functions with amplitudes decaying exponentially with decreasing energy. Such a distribution can be simulated via a convolution of a Gaussian function g and an exponential function h:.

$$g(E) = N \exp \frac{-E^2}{2\sigma^2}, \; h(E) = N \exp \frac{-E}{\varepsilon} \; . \qquad (3)$$

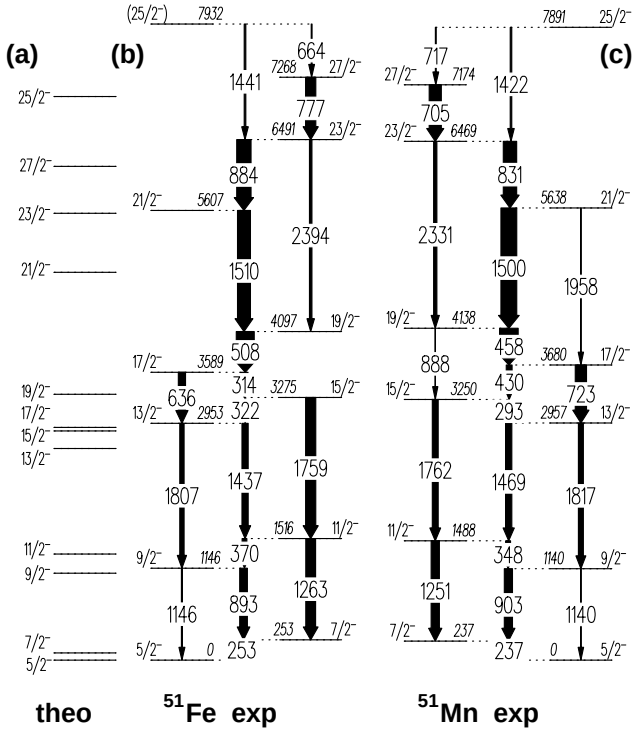

Fig. 2. Experimental level schemes of the $A = 51$ mirror nuclei obtained from the present analysis [parts (b) and (c)] compared with level energies obtained from a shell-model calculation [part (a)]. Energy labels are in keV.

N is a normalization constant, σ is related to the peak width according to $FWHM$=2.35·σ, and ε is related to the lifetime τ via eq. (2):

$$\varepsilon = E_0 \frac{v^2}{cd} \tau \qquad (4)$$

The convolution is done numerically, and from a standard χ^2 least-squares fit to the observed spectra ε, E_0 and N can be extracted. The peak width is a controlled parameter taken from a peak-width calibration. Figures 4(a) and (b) are the raw $2a1n$- and $2a1p$-gated spectra near the $17/2^- \rightarrow 13/2^-$ transitions detected in the 90° ring of Gammasphere. The raw spectra were used to avoid problems with background fluctuations following the subtracting of contaminating reaction channels. The peak to the left in fig. 4(a) and fig. 4(b) is the contaminating 622 keV transition from ^{52}Mn, and the 705 keV transition above the isomeric state in ^{51}Mn, respectively. The corresponding best fits are overlayed with a solid line. In fig. 4(b) a small Gaussian peak at 717 keV has also been included to account for the $25/2^- \rightarrow 27/2^-$ transition. The deduced lifetimes for these particular fits are τ=$2.6^{+2.9}_{-1.6}$ ns and τ=$1.92^{+0.23}_{-0.20}$ ns, respectively. Since the lifetimes of the low energy states in ^{51}Mn are known to be short [6], several transitions can be analysed below the $17/2^-$-states in the same way and one obtains weighted average lifetimes of $2.87^{+0.09}_{-0.11}$ ns for ^{51}Fe and $2.07^{+0.08}_{-0.07}$ ns for ^{51}Mn. The small uncertainty of the weigthed average lifetime in ^{51}Fe

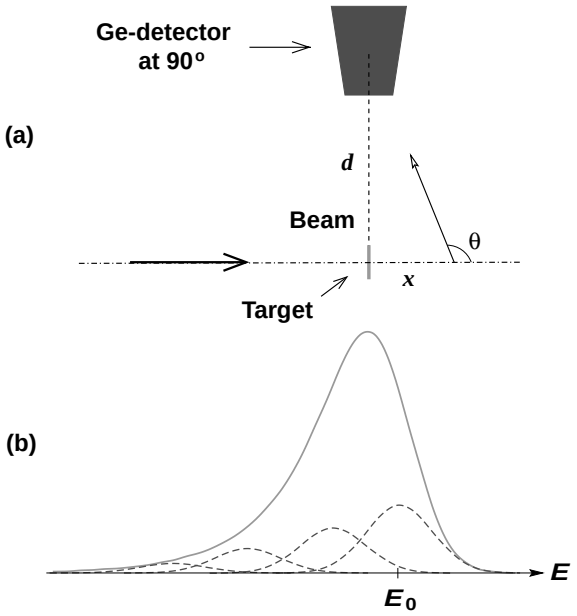

Fig. 3. Explanationary sketch for the nanosecond lifetime measurement. See text for details.

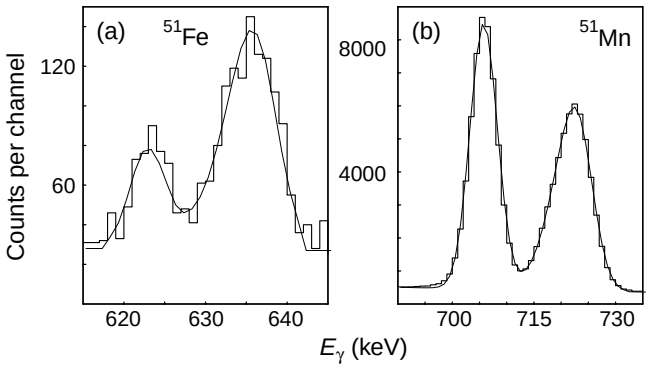

Fig. 4. Gamma-ray spectra near the $17/2^- \rightarrow 13/2^-$ transitions detected in the 90° ring of Gammasphere. The best lifetime fits are overlayed with a solid line. See text for details.

arises mainly from the measurement of the 253 keV transition, for which the uncertainty was found to be in the same order as for the ^{51}Mn transitions. A systematic uncertainty of about 15% in the deduced lifetimes arises from uncertainties in the kinematical factor $v/c = 0.041(2)$ and the average distance between the target and the interacting point in the Ge-detector, $d = 27.5(30)$ cm.

In fig. 5 the difference in level energy for mirror states between ^{51}Fe and ^{51}Mn (the so-called Coulomb Energy Difference, CED) is plotted. The diagrams can be understood qualitatively by means of different and changing numbers of proton holes in the levels of ^{51}Fe and ^{51}Mn, similar to lighter mirror nuclei systems [2,3]. The following discussion focusses on the signature $r = +i$ sequence, but is analogues for the $r = -i$ sequence. The $A = 51$ mirror nuclei start off moderately prolate deformed with one neutron hole (^{51}Fe) and one proton hole (^{51}Mn) in the [312]5/2 Nilsson orbit. The bands terminate in $19/2^-$

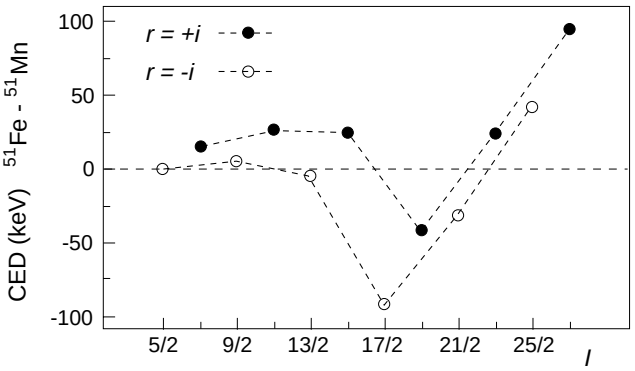

Fig. 5. Coulomb Energy Difference (CED) diagram for the $A = 51$ nuclei. Filled circles mark states with signature $r = +i$, open circles states with signature $r = -i$.

states, which corresponds to the maximum spin of the three-hole configurations $\nu^{-1} \otimes \pi^{-2}$ (^{51}Fe) and $\pi^{-1} \otimes \nu^{-2}$ (^{51}Mn), respectively in the $f_{7/2}$ shell. The breaking (and alignment) of the proton-hole pair in ^{51}Fe increases the average distance between protons, reducing the repulsive Coulomb force, and the binding energy increases relative to the corresponding states in ^{51}Mn. Consequently, the CED reaches a minimum at $I = 19/2$ as observed. To reach the terminating state at $I = 27/2$ the breaking of another hole pair is necessary. The configurations are $\nu^{-3} \otimes \pi^{-2}$ (^{51}Fe) and $\pi^{-3} \otimes \nu^{-2}$ (^{51}Mn). The principle is the same as above but in this case the proton-hole pair is broken in ^{51}Mn. As a concequence the CED increases between $I = 19/2$ and $I = 27/2$. It is interesting to note that the CED curves for the two signatures are split over the whole spin range, *i.e.*, the $r = -i$ sequence is energetically favoured in ^{51}Fe compared to ^{51}Mn. For a more quantitative description of the CED we refer to ref. [11].

Using the deduced branchings for the $17/2^- \rightarrow 13/2^-$ mirror transitions, *i.e.*, 52(3)% for ^{51}Fe and 64(3)% for ^{51}Mn, one obtains nearly identical $B(E2; 17/2^- \rightarrow 13/2^-)$ values for the two nuclei, namely 0.12(3) W.u. Shell-model calculations were performed to understand the nature of this isomerism. The full fp space was truncated to two-particle two-hole excitations across the shell gap at particle number 28, and the FPD6 residual interaction [19] was used, but with modified single-particle energies and effective operators as described in ref. [18].

Though quenched by roughly 1 MeV at the highest observed excitation energies, the predicted level sequence, in particular the inversion of the $25/2^-$ and $27/2^-$ states, is in nice agreement with experiment (see fig. 2). Moreover, the calculated branching ratios of the many parallel(mixed) dipole and quadrupole transitions match almost perfectly the observations. This manifests itself in a mean branching deviation (MBD) [20] of only MBD=0.15 [21]. The only major discrepancy is the $E2$ branch from the isomeric $17/2^-$ state, which is calculated to 84% in contrast to the observed 52 (3)%, which is caused by a theoretical $B(E2)$ value of 0.2 W.u. which is almost twice as large as measured. The lifetime of the $17/2^-$ state, however, is nicely reproduced with a calculated value of 2.9 ns. In this simple shell-model approach, the major origin of the isomerism are $\Delta I > 2$ spin gaps between most of the leading configurations of the initial and final state. The additional observed hindrance may be attributed to the different shapes of the two states, namely from (nearly) spherical ($17/2^-$) to moderately prolate ($13/2^-$). The shape of the latter cannot be predicted with the present simple approach, because deformation is created by multiple particle-hole excitations across the shell gap [2,11]. A similarly pronounced shape change is probably also occuring between the $19/2^-$ and $15/2^-$ states, but covered by the strong ($B(M1) \sim 0.4$ W.u.) $\Delta I = 1$ spin-flip transition between the $19/2^-$ and $17/2^-$ states, which contain large identical proton- and neutron-hole subconfigurations coupled to $I = I_{\max} = 19/2$ and $I = I_{\max} - 1 = 17/2$ within the seniority $v = 3$ scheme.

To summarize we identified 18 previously unknown γ-ray transitions in ^{51}Fe, which define a level scheme up to the terminating $27/2^-$-state. The previously known transitions of ^{51}Mn were confirmed, and weak transitions were added [17]. The level schemes of the $A = 51$ mirror nuclei reveal expected similarities and the small differences in energy due to the Coulomb interaction can be qualitatively understood by means of breaking and aligning of proton-hole pairs. The $17/2^-$-state in ^{51}Fe was found to be isomeric with a measured lifetime of τ=$2.87^{+0.09}_{-0.11}$±0.43 ns. The lifetime of the corresponding state in ^{51}Mn was measured to τ=$2.07^{+0.08}_{-0.07}$±0.31 ns, which is in agreement with the previous result [9].

The investigation of mirror nuclei has so far been limited to comparisons of level schemes, *i.e.* CED-diagrams. In this paper we also include lifetimes of isomeric states. However, there are attempts to extend the mirror symmetry discussion to other electro-magnetic decay properties such as precise branching and multipole mixing ratios [21]. This will give rise to investigations on how such observables depend on effective operators, *i.e.* on effective charges and effective g-factors [21].

The authors thank the ATLAS operating crew for their assistance. This research was supported in part by the Swedish Natural Science Research Councils and the U.S. Department of Energy under grant No. DE-FG05-88ER40406.

References

1. C.A. Ur et al., Phys. Rev. C **58**, 3163 (1998).
2. M.A. Bentley et al., Phys. Lett. B **437**, 243 (1998).
3. C.D. O'Leary et al., Phys. Rev. Lett. **79**, 4349 (1997).
4. H. Junde, Nucl. Data Sheets **87**, 507 (1999).
5. D. Rudolph et al., Z. Phys. A **358**, 379 (1997).
6. J.W. Noe et al., Nucl. Phys. A **277**, 137 (1977).
7. G. Fortuna et al., Nucl. Phys. A **299**, 479 (1978).
8. J.A. Cameron et al., Phys. Rev. C **44**, 2358 (1991).
9. J.W. Noe and P .Gural, *International Conference on Medium-Light Nuclei*, edited by P. Blasi and R.A. Ricci, (Florence, Italy, 1978) p. 459.
10. D. Mueller et al., Phys. Rev. C **15**, 1282 (1977).
11. M.A. Bentley et al., submitted to Phys. Rev. C.
12. I.-Y. Lee, Nucl. Phys. A **520**, 641c (1990).

13. M. Devlin et al., Nucl. Instrum. Meth. A **383**, 506 (1996).
14. D.G. Sarantites et al., Nucl. Instrum. Meth. A **381**, 418 (1996).
15. D.G. Sarantites et al., to be published.
16. C.E. Svensson et al., Nucl. Instrum. Meth. A **396**, 228 (1997).
17. J. Ekman et al., to be published.
18. D. Rudolph et al., Eur. Phys. J. A **4**, 115 (1999).
19. W.A. Richter, M.G. van der Merwe, R.E. Julies, and B.A. Brown, Nucl. Phys. A **523** 325 (1991).
20. D. Rudolph, K.P. Lieb, and H. Grawe, Nucl. Phys. A **597** 298 (1996).
21. J. Ekman et al., *Proceedings of the International Workshop on N=Z nuclei*, to be published.